



Quenching behavior in Nd³⁺ doped zinc phosphate glasses for near infrared laser applications

B. Venkata Rao^{1,3}, R. Jeevan Kumar^{*2,3}, C. Balanarayana¹

¹Loyola Degree College, Pulivendula-516 390, A.P., India

²Department of Physics, Sri Krishnadevaraya University, Anantapur- 517 003, A.P., India

³Department of Physics, JNTU University, Anantapur-515 002, A.P., India

Abstract : With interest in the luminescence properties, neodymium doped six series of zinc phosphate glass composition with different concentrations (0.1, 0.3, 0.5, 1.0, 1.5 and 2.0 mol%) were prepared by melt quenching method, and their luminescence has been investigated. Structural properties were accomplished from XRD (X-Ray Diffractometer) and Raman spectrum. Spectroscopic properties were investigated by measuring optical absorption spectrum, emission spectra and decay profiles. Neodymium environment in zinc phosphate host glass matrix can be accessed by Judd-Ofelt (J-O) theoretical approach. This theory gives three important parameters such as Ω_2 , Ω_4 and Ω_6 parameters. In turn these parameters were further used to calculate emission properties of Nd³⁺ ions. Luminescence parameters such as effective bandwidth ($\Delta\lambda_{\text{eff}}$), stimulated emission cross-sections (σ_p) and branching ratios (β_{exp}) have been studied through photoluminescence spectra. By adjusting the doping concentration in glass system, the concentration quenching phenomenon occurs. The photoluminescence spectra exhibit three prominent transitions. Of which, the near infrared transition located at 1.06 μm has high emission intensity. Further, decay time constants have been estimated from the decay profiles of Nd³⁺ doped different zinc phosphate glasses. This approach shows the present prepared zinc phosphate glasses significant for NIR lasing action.

Key words : Rare earth doped glasses; Zinc phosphate glasses; Neodymium; Judd-Ofelt theory; Absorption; Decay profiles.

1. Introduction

Recently, there has been a great deal of attention among scientists in searching the new materials especially, glasses doped with rare earth (RE) metal ions. Further, a lot of attention was paid to choose a suitable composition for the host matrix in which the RE ions can be introduced for obtaining a high luminescence signal. The latter may be useful for their applications in temperature sensors. When materials show high transparency in the visible and near-infrared spectral regions possessing low phonon energy with relatively high solubility of rare-earth elements in the matrix, they could act as promising materials in photonic devices applications [1].

Zinc oxide (ZnO) based materials has been extensively studied by researchers, scientists and industries, and found to be a potential candidate for various applications like solar cells, sensors and light emitting diodes. One of the advantages with ZnO is that it easily makes the coordination with several metal ions such as Aluminum, Fluorine, Gallium, Manganese and Neodymium ions [2]. The additions of alkalis to these zinc

phosphate (ZP) glasses are responsible for the non-linear variation of properties. This is really a remarkable change in the properties and has future key applications in optoelectronic and photonic devices. Due to the addition of alkalis internal friction, dielectric loss, viscosity and glass transition etc also varies. ZP glasses become more attractive because of their special physical properties such as high stability and low phonon energies [3]. In addition to the above, they are non-hygroscopic in nature and transparent from visible to IR regions. The addition of alkali fluorides to ZP glass decreases the phonon energies by modifying the glass structure and by increasing the mechanical strength of the glass. There are several articles published on the preparation of zinc based glasses [4,5] and still an emerging field of research and development.

Several rare earth (RE) ions have been studied for laser application. In order to improve the optical properties of ZP glasses, neodymium oxide is used as a dopant due to its unique optical properties. Among them, the Nd^{3+} ion is one of the most investigated, mainly due its large cross-sections of optical absorption near 800 nm ($^4\text{I}_{9/2} \rightarrow ^2\text{H}_{9/2} + ^4\text{F}_{5/2}$), which turn easiest the excitation by diode laser, and the high quantum efficiency of the $^4\text{F}_{3/2} \rightarrow ^4\text{I}_{11/2}$ emission near 1060 nm. Moreover, as the $^4\text{I}_{11/2}$ energy level is 2000 cm^{-1} above the ground state, this turn the system as four level one, which it is well known to favor the population inversion avoiding the re-absorption effect [6]. Lasing has been obtained in different bulk glasses doped with Nd^{3+} ions.

It will be of great interest to make detailed investigation on spectroscopic and luminance properties in the prepared ZP material as the rare earth dopant (Nd) can impart near infrared properties. Therefore, in the present study, high quality Nd^{3+} doped ZP glasses with various molar concentrations (0.1, 0.3, 0.5, 1.0, 1.5, and 2.0 mol%) were prepared by melt quenching techniques. The various key properties of the prepared Nd^{3+} doped ZP glasses like structural, optical, radiative and luminescence were investigated such as: structural by X-ray diffraction, Raman spectrum and optical properties by UV-Vis-NIR spectrophotometer. In case of radiative and luminescence properties, we have calculated parameters such as radiative transition probability (A_R), radiative lifetimes (τ_R), branching ratios (β_{cal}), stimulated emission cross-sections (σ_P) and experimental lifetimes (τ_{exp}) by theoretical and experimental data and then discussed.

2. Experimental techniques

Different zinc phosphate (ZP) glasses were prepared by using raw materials (99.9%), ammonium phosphate ($\text{NH}_4\text{H}_2\text{PO}_4$), lithium fluoride (LiF), strontium oxide (SrO), zinc oxide (ZnO) and dysprosium oxide (Nd_2O_3). Final glass compositions of the prepared glass samples are labelled as follows (mol%):

| | | |
|---|------|--|
| 1 | Nd01 | 59.9 $\text{NH}_4\text{H}_2\text{PO}_4$ -10LiF-10SrO-20ZnO-0.1 Nd_2O_3 |
| 2 | Nd03 | 59.7 $\text{NH}_4\text{H}_2\text{PO}_4$ -10LiF-10SrO-20ZnO-0.3 Nd_2O_3 |
| 3 | Nd05 | 59.5 $\text{NH}_4\text{H}_2\text{PO}_4$ -10LiF-10SrO-20ZnO-0.5 Nd_2O_3 |
| 4 | Nd10 | 59.0 $\text{NH}_4\text{H}_2\text{PO}_4$ -10LiF-10SrO-20ZnO-1.0 Nd_2O_3 |
| 5 | Nd15 | 58.5 $\text{NH}_4\text{H}_2\text{PO}_4$ -10LiF-10SrO-20ZnO-1.5 Nd_2O_3 |
| 6 | Nd20 | 58.0 $\text{NH}_4\text{H}_2\text{PO}_4$ -10LiF-10SrO-20ZnO-2.0 Nd_2O_3 |

Precise amounts of the starting materials in mol% were weighed out and ground in an agate mortar to obtain homogeneous mixtures. The mixtures were placed in porcelain crucible and then heated in an electric furnace. After heating, the obtained liquid was poured on brass plate and then pressed by another brass plate. The obtained glasses were used for characterization. Amorphous nature of the prepared glasses was verified by SEIFERT X-RAY diffractometer. Raman spectrum has recorded JASCO spectrometer. The optical absorption spectral measurements were collected using JASCO-670 double beam spectrophotometer in UV-VIS and NIR regions. The excitation, photoluminescence spectra and decay curves of Nd^{3+} doped glass samples were recorded using FLS-980 fluorescence spectrometer with 808 nm laser diode as excitation source.

3. Results and discussion

3.1. XRD analysis

The X-ray diffraction (XRD) profile for 0.5 mol% of Nd^{3+} doped ZP glass matrix is shown in Fig. 1. The analysis of the profiles shows no sharp diffraction peak, but a broad hump can be observed reflecting a

characteristic of amorphous material. From this figure, it is apparent that no characteristic diffraction peaks, indicating that the prepared glass is amorphous in nature.

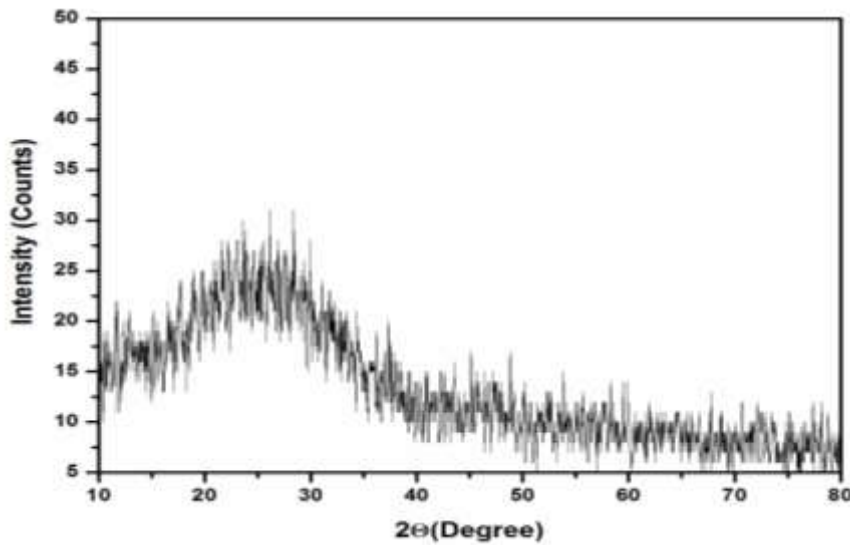


Fig.1. XRD pattern for 0.5 mol% Nd³⁺ doped zinc phosphate glass matrix

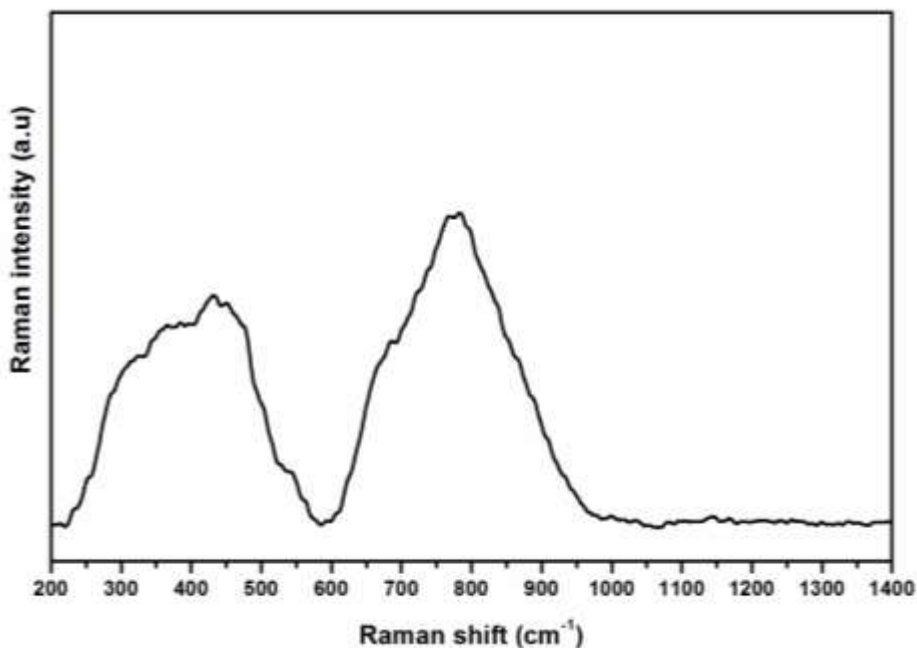


Fig.2 Raman spectrum of 0.5 mol% Nd³⁺ doped zinc phosphate glass matrix

3.2. Raman spectrum

Fig.2 shows Raman spectrum of 0.5 mol% of Nd³⁺ doped ZP glass matrix. The low frequency band extended from 300-480 cm⁻¹ region is related to the bending motion of phosphate polyhedral PO₄ units with cations like ZnO and SrO etc. as the modifiers. The broad band at 773 cm⁻¹ is due to symmetric stretching of (P-O-P) bridging oxygen bonds in (P₂O₇)⁴⁻ units. [7-9]. This peak is a convolution of two peaks i.e. one may be due to vibrations of the two joined Q² units and the second one to those of Q¹ units. Presence of last two bands indicates that due to addition of different modifiers into glass matrix, long range order of network become cut down and formed chain like units. This type of structural units increases glass strength.

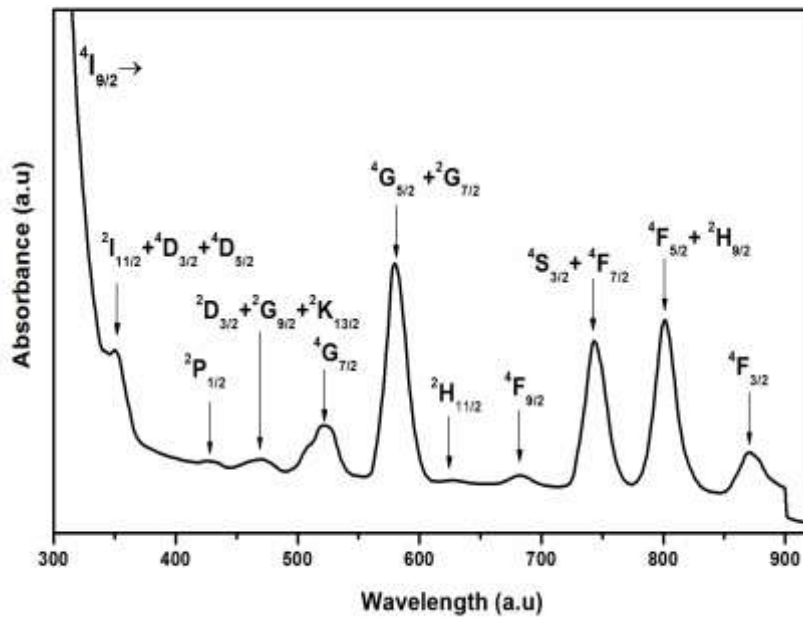


Fig.3. Absorption spectrum of 0.5 mol% Nd³⁺ doped zinc phosphate glass matrix

3.3. Absorption spectrum and Judd-Ofelt theory

Absorption spectrum of 0.5 mol% of Nd³⁺ doped ZP glass sample in the region of wavelength 350–920 nm is displayed in Fig. 3. The observed thirteen absorption bands, which originated from the ground state ⁴I_{9/2} to higher states assigned to different transitions of Nd³⁺ ions by comparing the peak positions with reported literature [10]. The position of these absorption transitions of Nd³⁺ zinc phosphate glass matrix located at 350, 430, 471, 526, 583, 621, 681, 746, 801 and 873 originates from the ⁴I_{9/2} ground state to the various excited states of Nd³⁺ such as ²I_{11/2}+⁴D_{3/2}+⁴D_{5/2}, ²P_{1/2}, ²D_{3/2}+²G_{9/2}+²K_{13/2}, ⁴G_{7/2}, ⁴G_{5/2}+²G_{7/2}, ²H_{11/2}, ⁴F_{9/2}, ⁴S_{3/2}+⁴F_{7/2}, ⁴F_{5/2}+²H_{9/2} and ⁴F_{3/2} respectively. The absorption band of Nd³⁺ located at ~580 nm corresponds to the hypersensitive transition which is dominated in intensity than other transitions of Nd³⁺ ions. It is noted that, in the UV-VIS-NIR region, the absorption bands of different transition levels overlap each other due to the presence of closed energy levels in Nd³⁺ ions and this difficulties arises can be resolved by addition of both the dipole strengths and the squared reduced matrix elements of overlapping transitions. The corresponding reduced matrix elements have been also added.

The Judd-Ofelt (J-O) theory [11, 12] is used to characterize radiative transitions for Nd³⁺ doped glasses. It gives three set of intensity parameters, Ω_λ ($\lambda=2, 4$ and 6), that are sensitive to the around the environment of the neodymium ions. The experimental oscillator strengths, f_{exp} , of the absorption bands can be calculated by

$$f_{\text{exp}} = 4.32 \times 10^{-9} \int \epsilon(\nu) d\nu$$

where $\epsilon(\nu)$ is the molar extinction coefficient. According to the Judd-Ofelt theory (J- O), the spectral intensity of an electric dipole absorption transition can be defined from the initial state, aJ to the final state, bJ'.

$$f_{\text{cal}}(aJ, bJ') = \frac{8\pi^2 mc \nu}{3hc^2 (2J+1)} \left[\frac{(n^2 + 2)^2}{9n} \right] \sum_{\lambda=2,4,6} \Omega_\lambda \left| \langle aJ \| U^\lambda \| bJ' \rangle \right|^2$$

In the above equation, all symbols are as usual meaning. The Judd-Ofelt intensity parameters Ω_λ are obtained from the experimental absorption band. The root mean square (RMS) deviation value of 0.52×10^6 is

obtained between the experimental and calculated oscillator strengths, indicates that good fit between two magnitudes and also good consistency of J-O intensity parameters. These results are shown in Table 1. It is observed that order of Ω_λ parameters is $\Omega_2 > \Omega_6 > \Omega_4$ for the Nd05 glass matrix. High Ω_2 parameter and low $\Omega_{4,6}$ parameters related to covalency and rigidity respectively is also observed.

Table 1 Experimental (f_{exp}) and calculated (f_{cal}) spectral intensities ($\times 10^{-6}$) of different absorption bands and Judd-Ofelt intensity parameters (Ω_λ , $\times 10^{-20} \text{ cm}^2$) for Nd05 zinc phosphate glass matrix

| S.NO | Transition | f_{exp} | f_{cal} |
|---------------|--------------------------------------|------------|-----------|
| 1 | $^2I_{11/2} + ^4D_{3/2} + ^4D_{5/2}$ | 0.75 | 0.82 |
| 2 | $^2P_{1/2}$ | 0.62 | 0.62 |
| 3 | $^2K_{13/2} + ^2G_{9/2} + ^2D_{3/2}$ | 1.91 | 1.99 |
| 4 | $^4G_{7/2}$ | 3.91 | 4.10 |
| 5 | $^4G_{5/2} + ^2G_{7/2}$ | 21.20 | 22.11 |
| 6 | $^2H_{11/2}$ | 0.11 | 0.12 |
| 7 | $^4F_{9/2}$ | 1.10 | 1.15 |
| 8 | $^4S_{3/2} + ^4F_{7/2}$ | 6.90 | 6.99 |
| 9 | $^4F_{5/2} + ^2H_{9/2}$ | 6.35 | 6.98 |
| 10 | $^4F_{3/2}$ | 1.84 | 2.10 |
| RMS deviation | | ± 0.52 | |
| Ω_2 | | 6.11 | |
| Ω_4 | | 4.23 | |
| Ω_6 | | 5.54 | |

Table 2 : Radiative transition probabilities (A_R) (s^{-1}), total transition probabilities (A_T), branching ratios (β_R), and radiative lifetimes (τ_R) (μs) of certain excited levels for Nd05 zinc phosphate glass matrix

| SLJ | S'L'J' | A_R | β_R | |
|------------------|--------------|-------|-----------|--------------------------------|
| $^4F_{3/2}$ → | $^4F_{15/2}$ | 16 | 0 | $A_T = 3636$ $\tau_R = 275$ |
| | $^4I_{13/2}$ | 349 | 9 | |
| | $^4I_{11/2}$ | 1827 | 51 | |
| | $^4I_{9/2}$ | 1444 | 40 | |

Table 3 : Emission band positions (λ_p , nm), effective bandwidths ($\Delta\lambda_{eff}$, nm), radiative transition probabilities (A , s^{-1}), peak stimulated emission cross-sections (σ_p , $\times 10^{-20} \text{ cm}^2$) and branching ratios (β_{exp} , %) of emission transitions for Nd05 zinc phosphate glass matrix

| Parameters | $^4F_{3/2} \rightarrow ^4I_{9/2}$ | $^4F_{3/2} \rightarrow ^4I_{11/2}$ | $^4F_{3/2} \rightarrow ^4I_{13/2}$ |
|-----------------------|-----------------------------------|------------------------------------|------------------------------------|
| λ_p | 894 | 1059 | 1333 |
| $\Delta\lambda_{eff}$ | 48 | 30 | 57 |
| A_R | 1444 | 1827 | 349 |
| σ_p | 1.15 | 2.48 | 0.85 |
| β_{exp} | 37 | 58 | 5 |

J-O intensity parameters are further used to evaluate the different radiative properties like radiative transition probability (A_R), radiative lifetime (τ_R) and branching ratios (β_R), of certain excited states are calculated for Nd05 glass matrix and are collected in Table 2 for $^4F_{3/2}$ state of Nd^{3+} .

The radiative lifetimes (τ_R) and branching ratios (β_R) can be calculated using the equations

$$\tau_{rad} = \frac{1}{\sum_{bJ'} A_{rad}(aJ, bJ')^{-1}}$$

$$\beta_R(aJ, bJ') = \frac{A_{rad}(aJ, bJ')}{\sum_{bJ'} A_{rad}(aJ, bJ')}$$

It is noticed (from Table 2) that the ${}^4F_{3/2} \rightarrow {}^4I_{11/2}$ transition has more A_R magnitude and branching ratios (β_{cal}).

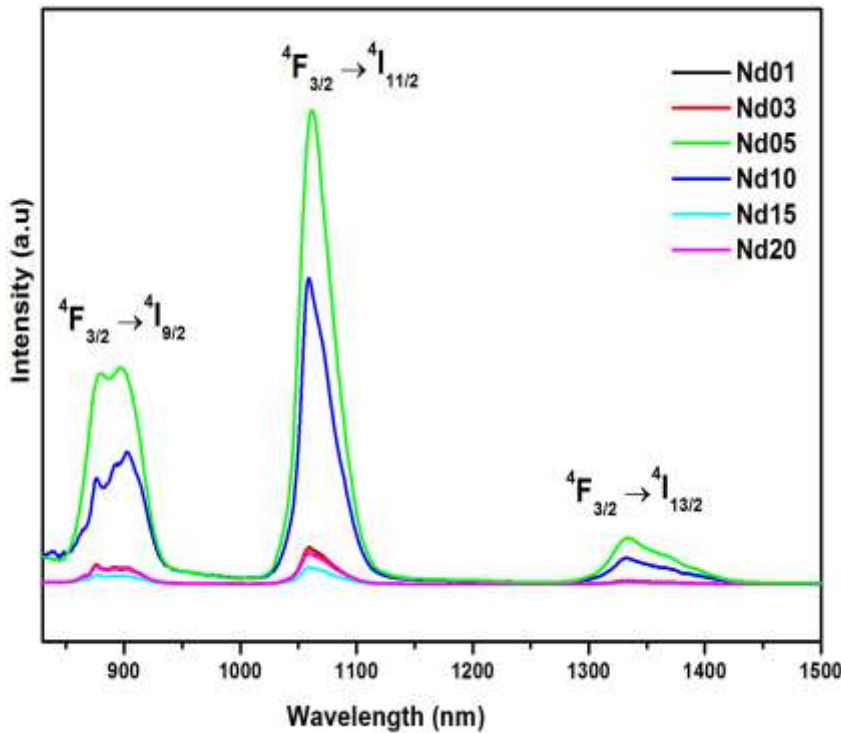


Fig.4 Emission spectra of Nd³⁺ doped zinc phosphate glass matrix with different concentrations

3.4. Near infrared emission properties

Fig. 4, shows the luminescence emission spectra of Nd³⁺ doped ZP glass matrix for Nd01, Nd03, Nd05, Nd10, Nd15 and Nd20 glasses in the range of wavelength 800–1300 nm under the excitation of 808 nm laser diode. In the present study, three emission peaks are observed at 894, 1059 and 1333 nm corresponding to ${}^4F_{3/2} \rightarrow {}^4I_{9/2}$, ${}^4F_{3/2} \rightarrow {}^4I_{11/2}$ and ${}^4F_{3/2} \rightarrow {}^4I_{13/2}$ transitions, respectively. From the emission spectra, it is clearly observed that emission intensities increases upto 0.5 mol% of neodymium and then decreases with the increase of Nd³⁺ concentration. This is due to concentration quenching. It is occur due to the increasing of non-radiative (NR) energy transfer through cross relaxation and resonant energy channels among Nd³⁺ ions [13].

From Fig.4, the most intense emission is observed for the ${}^4F_{3/2} \rightarrow {}^4I_{11/2}$ near infrared transition than other emission transitions. From the emission spectra, the intensity of probable lasing transition can be assessed, like the effective line widths (λ_{eff}), branching ratio (β_{exp}), from area under the emission band, and peak stimulated emission cross-sections (σ_p) for the certain transitions, ${}^4F_{3/2} \rightarrow {}^4I_J$ (J =9/2, 11/2 and 13/2).

The peak stimulated emission cross-section (σ_p)

$$\sigma_p(aJ, bJ') = \frac{\lambda_p^4}{8\pi c n^2 \Delta\lambda_{eff}} A_{rad}(aJ, bJ')$$

where λ_p is emission peak wavelength and $\Delta\lambda_{eff}$ is the effective linewidth.

The higher σ_p is very important property for laser application. From the three emission transitions of Nd³⁺ ion, ${}^4F_{3/2} \rightarrow {}^4I_{11/2}$ transition has higher σ_p than rest of transitions and among all concentrations of Nd³⁺, Nd05 zinc phosphate glass matrix shows higher σ_p i.e. $2.48 \times 10^{-20} \text{ cm}^2$. The value of σ_p for the ${}^4F_{3/2} \rightarrow {}^4I_{11/2}$ near infrared transition of the Nd05 glass matrix located at 1.06 μm is found to be high. Hence, the glass Nd05 glass matrix might be useful for near infrared lasing material through ${}^4F_{3/2} \rightarrow {}^4I_{11/2}$ transition.

The β is one of the important and attractive parameter to determine lasing power of a particular transition and it is well established that an emission transition having the values of β is greater than 50% is can be considered as more as potential for laser emission. The experimental branching ratios (β_{exp}) are measured under the relative areas of the each individual emission transitions and it is found to be higher for ${}^4F_{3/2} \rightarrow {}^4I_{11/2}$ transition. In the present study, it is observed that there is a good agreement between β_{exp} and β_R .

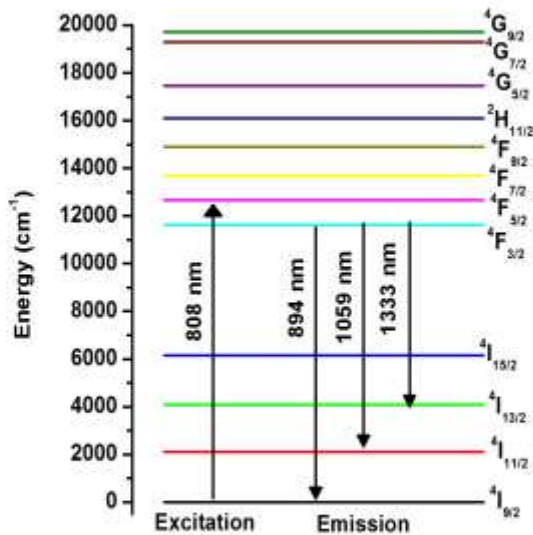


Fig.5 Energy level scheme of Nd^{3+} doped zinc phosphate glass matrix

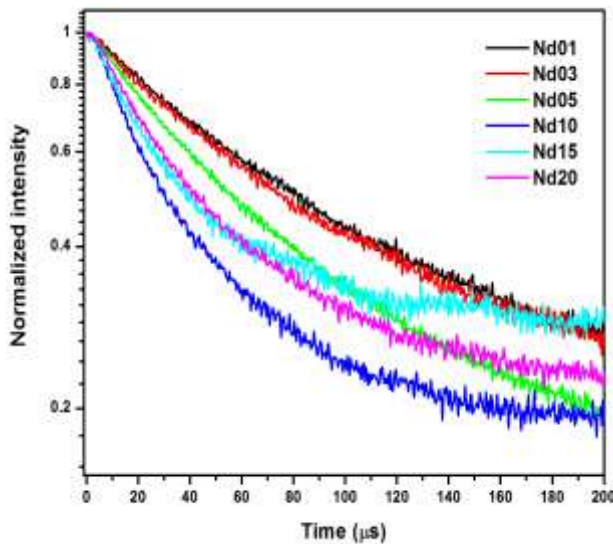


Fig.6 Decay profiles for various concentrations of Nd^{3+} doped of zinc phosphate glasses

3.5. Decay kinetics

With 808 nm excitation, into the ${}^4I_{9/2} \rightarrow {}^4F_{5/2} + {}^2H_{9/2}$ absorption (excitation) band and then the ${}^4I_{13/2} \rightarrow {}^4F_{9/2}$ transition is more favourable way to depopulate nonradiatively through the multiphonon relaxation (MPR) due to the fact that the energy gap between them is low. No emissions from other energy levels are expected. The

MPR from the ${}^4F_{9/2}$ level is negligible owing to fact that the next level (${}^6F_{1/2}$) lies lower by about $\sim 6900\text{ cm}^{-1}$. This wide energy gap between the ${}^4F_{9/2} \leftrightarrow {}^6F_{1/2}$ levels leads to a high quantum efficiency of the ${}^4F_{9/2}$ emitting level [6] and emission takes place from this level as shown in Fig. 5 energy level diagram.

The fluorescence decay profiles for ${}^4F_{3/2}$ level of Nd^{3+} doped zinc phosphate glasses with the variation of Nd^{3+} content while maintaining with a fixed emission at $1.06\ \mu\text{m}$, which corresponds to the electronic transition (${}^4F_{3/2} \rightarrow {}^4I_{11/2}$) and excitation at 808 nm is displayed in Fig. 6. Fluorescence lifetimes were measured from e-folding time of the emission intensities. For the decay curves which are bi-exponential behavior, the resultant decay lifetime can be calculated using the formula [14]

$$I(t) = A_1 \exp\left(\frac{-t}{\tau_1}\right) + A_2 \exp\left(\frac{-t}{\tau_2}\right)$$

where 'I' is the photoluminescence intensity at any time 't' after switching off the excitation illumination, τ_1 and τ_2 are fast and slow decay times respectively, A_1 , A_2 are respective fitting (weighing) parameters. The first term in the equation refers to excited state absorption and second term refers to the energy transfer (ET) process or in other words radiative and non-radiative decays.

The experimental lifetimes (τ_{exp}) have been evaluated using the relation

$$\tau_{\text{exp}} = \frac{A_1 \tau_1^2 + A_2 \tau_2^2}{A_1 \tau_1 + A_2 \tau_2}$$

It is observed that the decay lifetimes decreases with increasing neodymium content in the ZP glass system. The lifetimes were found to be 910, 895, 800, 745, 693 and 580 μs for the Nd01, Nd03, Nd05, Nd10, Nd15 and Nd20 ZP glasses respectively. The decay lifetime decreases from 910 μs to 580 μs . This gradual decrease in lifetime is consistent with the steady state luminescence behavior which is due to the increase in non-radiative transition processes to excited states of Nd^{3+} ions. However, the lifetime value drops to 580 μs when Nd^{3+} content increases to 2.0 mol% which might be due to the larger amount of activator ions in the glass system. Except Nd01, Nd03 and Nd05 glasses, all ZP glasses of decay profiles are fitted non-exponential function at short times. This type of activity is due to energy transfer (ET) between two Nd^{3+} atoms and concentration quenching. In order to investigate the process involved in the ET mechanism, the non-exponential decay curves for the ${}^4F_{9/2}$ level of Nd^{3+} ions have been analyzed using Inokuti–Hirayama (I-H) model [15].

$$I(t) = I_0 \exp\left\{-t/\tau_0 - Q(t/\tau_0)^{3/S}\right\}$$

where t is the time, τ_0 is the intrinsic decay time of donors in the absence of acceptors, energy transfer parameter (Q). The Q value linked to variable interaction parameter, S and the gamma function $\Gamma(x)$ parameters. $\sqrt{\pi}$ is 1.77 (for S=6, dipole–dipole), 1.43 (for S=8, dipole–quadrupole) and 1.33 (for S=10, quadrupole–quadrupole). In co-doped system, decays were fitted to S=6. From this model it is assessed that ET occurs through dipole–dipole (d-d) interaction.

Conclusions

In the present study, neodymium doped six series of zinc phosphate glass composition with different concentrations (0.1, 0.3, 0.5, 1.0, 1.5 and 2.0 mol%) were prepared by melt quenching method, and their luminescence has been investigated. Structural properties were accomplished from XRD (X-Ray Diffractometer) and Raman spectrum. Spectroscopic properties were investigated by measuring optical absorption spectrum, excitation spectrum, emission spectra and decay profiles. Neodymium environment in zinc phosphate host glass matrix can be accessed by Judd-Ofelt (J-O) theoretical approach. It is observed that order of Ω_λ parameters is $\Omega_2 > \Omega_6 > \Omega_4$ for the zinc phosphate glasses. High Ω_2 parameter and low Ω_4 parameter related to covalency and rigidity respectively is observed. J-O intensity parameters are used to further to evaluate the different radiative properties like radiative transition probability (A_R), radiative lifetime (τ_R) and branching ratios (β) of certain excited states. It is noticed that the ${}^4F_{3/2} \rightarrow {}^4I_{11/2}$ transition has more A_R magnitude and branching ratios (β_{cal}). Luminescence parameters such as effective bandwidth ($\Delta\lambda_{\text{eff}}$), stimulated emission cross-sections (σ_p) and branching ratios (β_{exp}) have been studied through photoluminescence spectra. By adjusting the

doping concentration in glass system, the quenching was observed in emission intensity. The photoluminescence spectra exhibit three prominent transitions. Of which, the near infrared transition located at 1.06 μm has high emission intensity. Furthermore, it is also noticed that the present glass (Nd05) sample shows higher branching ratios, transition probability, and emission cross-sections for ${}^4\text{F}_{3/2} \rightarrow {}^4\text{I}_{11/2}$ transition. Further, decay time constants have been estimated from the decay profiles of Nd^{3+} doped different zinc phosphate glasses. PL decay lifetimes are determined by fitting the decay data with the mono exponential decay equation. The decay lifetimes decreases with increasing of Nd^{3+} concentration. This gradual decrease in lifetime is consistent with the steady state luminescence behavior which is due to the increase in non-radiative transition processes to excited states of Nd^{3+} ions. This approach shows the present prepared zinc phosphate glasses useful towards the development of near infrared lasing materials.

References

1. Y.K. Sharma, S.S.L. Surana, R.K. Singh, R.P. Dubedi, *Opt. Mater.* 29, (2007) 598–604.
2. V. Ganesh, I.S. Yahiaa, S. AlFaifya, Mohd. Shkira, *J. Phys. Chem. Solids* 100 (2017) 115–125.
3. R. Vijaya, V.Venkatramu, P. Babu, C.K. Jayasankar, U.R. Rodríguez-Mendoza, V. Lavin, *J. Non-Cryst. Solids* 365 (2013) 85-92.
4. D.D. Ramteke, R.E. Kroon, H.C. Swart, *J. Non-Cryst. Solids* 457 (2017) 157–163.
5. A. Srinivasa Rao, B. Rupa Venkateswara Rao, M.V.V.K.S. Prasad, J.V. Shanmukha Kumar, M. Jayasimhadri, J.L. Rao, R.P.S. Chakradhar, *Physica B* 404, (2009) 3717–3721.
6. F.B. Costa, K. Yukimitua, L.A.O. Nunesb, M.S. Figueiredoc, L.H.C. Andrade, S.M. Lima, J.C.S. Moraes, *J. Phys. Chem. Solids.* 88 (2016) 54–59.
7. J.E. Pemberton, L. Latifzadeh, J.P. Fletcher, S.H. Risbud, *Chem. Mater.*, 3 (1991) 195-200.
8. D. Ilieva, B. Jivov, G.Bogacev, C. Petkov, I. Penkov, Y.Dimitriev, *J. Non-Cryst. Solids*, 238 (2001) 195-202.
9. P. Stoch, W. Szczerba, W. Bodnar, M. Ciecinska, Agata Stochd, Eberhard Burkel, *Phys. Chem. Chem. Phys.*, 2014, 16, 19917—19927.
10. W.T. Carnall, H. Crosswhite, H.M. Crosswhite, Argonne National Laboratory Report
11. II, 1977
12. B.R. Judd, *Phys. Rev.* 127 (1962) 750.
13. G.S. Ofelt, *J. Chem. Phys.* 37 (1962) 511.
14. F. Zaman, G. Rooh, N. Srisittipokakun, S. Ruengsri, H.J. Kim, J. Kaewkhao, *J. Non-Cryst. Solids*, 452, (2016) 307–311.
15. T. Sasikala, L. RamaMoorthy, A. MohanBabu, T. SrinivasaRao, *J. Solid. State Chem.* 203 (2013) 55-59.
16. K. Linganna, Ch. Basavapoornima, C.K. Jayasankar, *Optics Commun.* 344 (2015) 100–105.
